EBioMedicine 30 (2018) 52–61

Contents lists available at ScienceDirect

EBioMedicine

journal homepage: www.ebiomedicine.com

Research Paper

Visual Restoration after Cataract Surgery Promotes Functional and Structural Brain Recovery

Haotian Lin [a,*,1,2], Li Zhang [a,b,1], Duoru Lin [a,1], Wan Chen [a], Yi Zhu [a,c], Chuan Chen [a,c], Kevin C. Chan [d,e], Yizhi Liu [a,*], Weirong Chen [a,*]

[a] State Key Laboratory of Ophthalmology, Zhongshan Ophthalmic Center, Sun Yat-sen University, Guangzhou, Guangdong 510060, People's Republic of China
[b] Department of Ophthalmology, The Central Hospital of Wuhan, Tongji Medical College, Huazhong University of Science and Technology, Wuhan, Hubei 430014, People's Republic of China
[c] Department of Molecular and Cellular Pharmacology, University of Miami Miller School of Medicine, Miami, FL 33136, USA
[d] NYU Eye Center, Department of Ophthalmology, NYU School of Medicine, NYU Langone Health, New York University, New York, NY 10016, USA
[e] Department of Radiology, NYU School of Medicine, NYU Langone Health, New York University, New York, NY 10016, USA

ARTICLE INFO

Article history:
Received 11 January 2018
Received in revised form 1 March 2018
Accepted 4 March 2018
Available online 7 March 2018

Keywords:
Brain plasticity
Vision restoration
Visual impairment
Age-related cataract

ABSTRACT

Background: Visual function and brain function decline concurrently with aging. Notably, cataract patients often present with accelerated age-related decreases in brain function, but the underlying mechanisms are still unclear. Optical structures of the anterior segment of the eyes, such as the lens and cornea, can be readily reconstructed to improve refraction and vision quality. However, the effects of visual restoration on human brain function and structure remain largely unexplored.

Methods: A prospective, controlled clinical trial was conducted. Twenty-six patients with bilateral age-related cataracts (ARCs) who underwent phacoemulsification and intraocular lens implantation and 26 healthy controls without ARC, matched for age, sex, and education, were recruited. Visual functions (including visual acuity, visual evoke potential, and contrast sensitivity), the Mini-Mental State Examination and functional magnetic resonance imaging (including the fractional amplitude of low-frequency fluctuations and grey matter volume variation) were assessed for all the participants and reexamined for ARC patients after cataract surgery. This trial was registered with ClinicalTrials.gov (NCT02644720).

Findings: Compared with the healthy controls, the ARC patients presented decreased brain functionality as well as structural alterations in visual and cognitive-related brain areas preoperatively. Three months postoperatively, significant functional improvements were observed in the visual and cognitive-related brain areas of the patients. Six months postoperatively, the patients' grey matter volumes in these areas were significantly increased. Notably, both the function and structure in the visual and cognitive-related brain areas of the patients improved significantly and became comparable to those of the healthy controls 6 months postoperatively.

Interpretation: We demonstrated that ocular reconstruction can functionally and structurally reverse cataract-induced brain changes. The integrity of the eye is essential for maintaining the structure and function of the brain within and beyond the primary visual pathway.

© 2018 The Authors. Published by Elsevier B.V. This is an open access article under the CC BY-NC-ND license (http://creativecommons.org/licenses/by-nc-nd/4.0/).

1. Introduction

Aging is accompanied by concurrent declines in visual and brain functions. Studies in humans and animal models provide converging evidence that these functional changes are often accompanied by specific structural alterations of the eye and brain regions (Knezovic et al., 2015; Hsu et al., 2016; Ferreira et al., 2017). The eyes and brain are anatomically and functionally connected (Ochoa-Urdangarain et al., 2001). On the one hand, the retina and optic nerve are extensions of the brain that can be directly observed from the surface of the body. On the other hand, as visual information accounts for a large proportion of brain inputs, visual skills, such as stereopsis and form perception, are highly and consistently correlated with intellectual development (Gottfried and Gilman, 1985).

Ocular diseases have been shown to contribute to cognitive decline and abnormal changes in brain structure. Subjects with untreated poor vision showed a 5- to 9·5-fold increased risk of developing Alzheimer's disease (AD) or other cognitive disorders (Rogers and

* Corresponding authors at: State Key Laboratory of Ophthalmology, Zhongshan Ophthalmic Center, Sun Yat-sen University, Guangzhou, Guangdong 510060, People's Republic of China.
E-mail addresses: gddlht@aliyun.com (H. Lin), yizhi_liu@aliyun.com (Y. Liu), chenwr_q@aliyun.com (W. Chen).
[1] These authors contributed equally to this work.
[2] Haotian Lin has been invited as a guest speaker to present part of this study at The Lancet-CAMS Health Summit 2016 in Beijing, China.

https://doi.org/10.1016/j.ebiom.2018.03.002
2352-3964/© 2018 The Authors. Published by Elsevier B.V. This is an open access article under the CC BY-NC-ND license (http://creativecommons.org/licenses/by-nc-nd/4.0/).

Langa, 2010). Impairment of the brain's short-range and long-range functional connections in visual pathways, the frontal cortex, visual areas, posterior parietal, and frontal cortices was also detected in children with anisometropic amblyopia (Wang et al., 2014). Furthermore, widespread structural abnormalities in the central nervous system extending beyond the visual cortex were observed in patients with advanced primary open-angle glaucoma, an irreversible disease involving the retina and optic nerve (Dai et al., 2013).

Age-related cataract (ARC), the most common cause of vision decline or loss in the general aging population, is due to lens opacification (Asbell et al., 2005). A retrospective study in Taiwan of 19,954 ARC patients revealed a marked increase in the overall incidence of AD after an 8-year follow-up, suggesting that ARC is associated with structural and functional impairments of the brain (Lai et al., 2014). The vision loss of most cataract patients can be readily corrected via phacoemulsification and intraocular lens (IOL) implantation. However, whether functional and structural changes in the brain can be reversed after visual restoration is largely unknown. Previous studies have reported cognitive improvements in elderly patients after cataract surgery (Tamura et al., 2004; Ishii et al., 2008). However, most of these functional analyses were based on subjective questionnaire investigations and lacked objective evidence, such as neuroimaging. Furthermore, whether ocular reconstruction can promote functional and structural changes in specific brain regions remains unclear.

In the present study, we conducted a prospective, controlled clinical trial with consecutive patients presenting bilateral ARC. These patients exhibited significantly decreased visual function and underwent phacoemulsification with IOL implantation. We measured changes in brain function and structure before and after cataract surgery using functional magnetic resonance imaging (fMRI), a well-established neuroimaging technology that not only evaluates grey matter (GM) variation but also detects functional changes in the brain by monitoring blood oxygen level-dependent signals (Tambini et al., 2017), and the Mini-Mental State Examination (MMSE), a classic measurement of cognitive impairment (Predictors, 2017; Dixon et al., 2017a). We demonstrate that patients with ARC display impaired brain function and structure, but these changes can be fully reversed by visual acuity restoration.

2. Materials and Methods

2.1. Participants and Study Design

Twenty-six patients (13 males and 13 females) with ARC and 26 healthy controls matched for age, sex, and education, were recruited from Zhongshan Ophthalmic Center (ZOC). Written informed consent was obtained from all participants or their legal guardians. This study was approved by the Ethics Committee of ZOC at Sun Yat-sen University and followed the tenets of the Declaration of Helsinki. Twenty-six patients (52 eyes) were allocated to the Tecnis ZMB00 IOL (Abbott Medical Optics, Santa Ana, CA, USA) or ZCB00 IOL (Abbott Medical Optics, Santa Ana, CA, USA) arms depending on the patient's choice. The inclusion criteria for the study were as follows: cataracts in both eyes classified according to the Lens Opacity Classification System III, corneal astigmatism < 1·0 diopters (D), and IOL power between +18·0 and +25·0 D. The exclusion criteria included a medical history of neurological or psychiatric disorders, prior refractive, glaucoma, or penetrating keratectomy surgery, degenerative optical diseases, associated ocular or systemic diseases that may interfere with the results, significant vitreous loss during surgery that may hamper the implantation and performance of IOLs, and anterior chamber hyphema. Cataract surgery was performed in all patients by the same experienced ophthalmologist (WRC). The standard technique in all patients consisted of sutureless phacoemulsification using a Legacy 2000 Series and Infinity phacoemulsification machine (Alcon Laboratories Inc., Fort Worth, Texas, USA), with clear corneal incisions up to 3·2 mm and 5·0 to 5·5 mm capsulorhexis. Surgery was performed on the second eye 1 month after the first procedure in each patient. Structural and functional MRI scans were performed before surgery and at 1 week, 3 months, and 6 months after surgery on the second eye (Fig. 1). This trial was registered with ClinicalTrials.gov, NCT02644720.

2.2. Examination of Ocular Structure and Visual Function

At the 6-month follow-up visit, a slit-lamp examination was performed to examine the transparency of the posterior capsule and to exclude residual posterior capsule plaques. The locations of the IOLs were

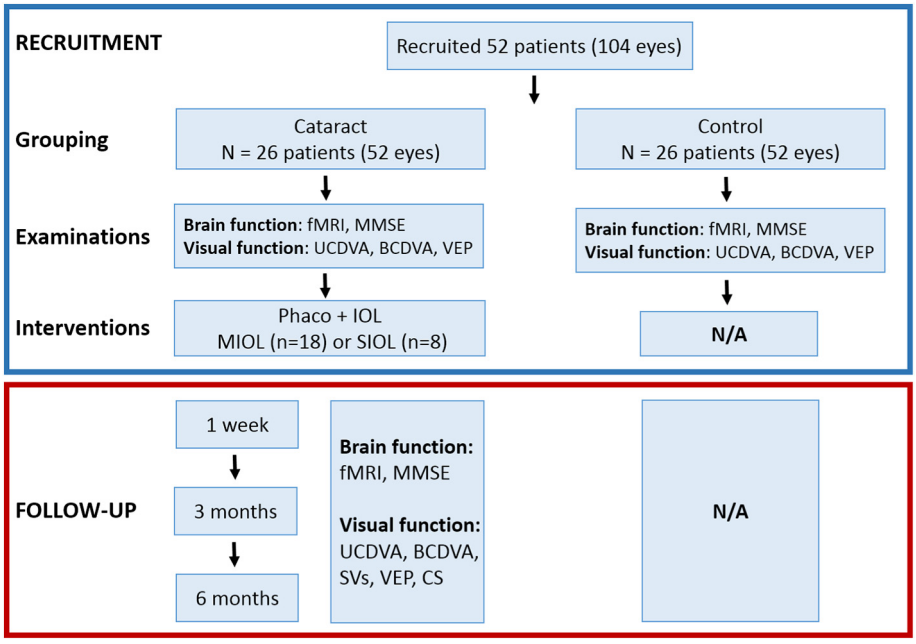

Fig. 1. Flowchart of recruitment and follow-up evaluations from 1 week after the second eye surgery. Notes: fMRI, functional magnetic resonance imaging; MMSE, Mini-Mental State Examination; UCDVA, uncorrected distance visual acuity; BCDVA, best-corrected distance visual acuity; CS, contrast sensitivity; SVs, straylight values; VEP, visual evoked potential; IOL, intraocular lens; SIOL, single-focus intraocular lens; MIOL, multifocal intraocular lens.

recorded by a slit lamp (BX900; HAAG-STREIT AG, Bern, Switzerland) examination and a 3-dimensional anterior segment imaging and analysis system (Pentacam HR; Oculus, Inc., Wetzlar, Germany). Distance visual acuity was examined with a Standard Logarithmic Visual Acuity E chart (Snellen). UCDVA (LogMAR) and BCDVA (LogMAR) were recorded preoperatively and at 1 week, 3 months, and 6 months postoperatively. For the correlation analysis between VA (UCDVA and BCDVA) and the fALFF value and GM volume, the VA data were calculated by averaging the binoculus.

Retinal SV measurements were obtained with a C-Quant straylight meter (Oculus Optikgerate GmbH, Wetzlar, Germany) (van der Meulen et al., 2012). The patient viewed a series of concentric areas. The smallest area in the center was divided into two halves. This area was the test field where the patient was asked to look when a concentric ring flickered with varying intensity. The flickering in the straylight source produced a certain amount of perceived flickering in the test field. The patient was asked to compare the two halves of the test field, one of which included additional counter-phase flickering, and to choose the side that flickered more strongly by pressing a button. The selected side defined a psychometric function from which the SV was obtained.

The PVEP was recorded using an Espion system (Diagnosys LLC, Lowell, MA, USA) in accordance with the International Society for Clinical Electrophysiology of Vision (ISCEV) recommendations (Odom et al., 2016). Frontal (Fz)-occipital (Oz) electrode placement was performed. Patient refractions were corrected with trial lenses using the international standard visual acuity chart before the PVEP was examined. All patients were instructed to maintain fixation at the center of a stimulus located at a distance of 1 m in front of a 20 × 30 cm black-and-white video display monitor (contrast 99%). The reversal rate was 1 reversal per second. The checkerboard stimulus subtended a visual angle of 5·7° vertically and 8·5° horizontally on either side of the fixation point. The P100 amplitude and latency for checkerboard sizes (15 min of arc) were recorded. An experienced electrophysiology technician closely monitored the fixation stability of the eyes. If the patient was not cooperative, the PVEP examination was repeated. All PVEP examinations were performed under the same laboratory conditions. For the correlation analysis between the peak time or amplitude and the fALFF value or GM volume, the average value for the binoculus was calculated.

CS was tested with a Contrast Glare Tester 1000 (Puell et al., 2006) (CGT-1000 Takagi Seiko Co., Ltd., Nagano, Japan) at 1 week, 3 months, and 6 months postoperatively. This instrument accurately determines CS in a simple and rapid fashion. The contrast threshold was presented at 12 levels, from 0·01 to 0·45, and was determined using a staircase procedure similar to that used in automatic visual field tests. The test was conducted at a distance of 35 cm from the screen and lasted approximately 1 min per eye. The patient was required to press a button only when he or she observed the stimulus. CS function was always determined by measuring best-corrected visual acuity to prevent residual refractive errors from affecting the CS value. The absolute value of log CS was used in the statistical analysis. For the correlation analysis between fALFF values and CS, the CS data were collapsed into a single index using the weighted mean contrast sensitivity (WMCS), which is defined as the mean of the data for each spatial frequency multiplied by the corresponding contrast sensitivity (Leguire et al., 2011).

2.3. Evaluation of Cognitive and Brain Functions

MMSEs were performed to evaluate cognitive function by trained clinical physicians. The MMSE contains 5 sections (orientation, registration, attention and calculation, recall and language). A higher MMSE score indicates better cognitive conditions (range 0 to 30). MRI evaluations were carried out using a MAGNETOM Verio 3 T MR scanner (A Tim System; Siemens, Erlangen, Germany). Resting-state fMRI scans were performed using an echo planar imaging sequence with the following parameters: repetition time = 3000 ms, echo time = 30 ms, flip angle = 90°, matrix = 64 × 64, field of view = 192 × 192 mm^2, slice thickness = 3 mm, and slice gap = 0·5 mm. Each brain volume was composed of 41 axial slices, and each functional run contained 124 volumes. During the scans, all subjects were instructed to look forward through the center of the mirror, fix their vision in that direction and minimize movement. Tight but comfortable foam padding was used to minimize head motion, and earplugs were used to reduce scanner noise. All subjects confirmed that they did not fall asleep during scanning. Structural T1-weighted images were acquired in the sagittal orientation using a magnetization-prepared rapid gradient echo imaging sequence with the following parameters: repetition time = 1900 ms, echo time = 2·52 ms, flip angle = 9°, acquisition matrix = 256 × 256, field of view = 250 × 250 mm^2, and 176 total images with 1-mm-thick slices. The scanning time was 258 s.

2.4. Data Preprocessing

Standard data processing software, Data Processing Assistant for Resting-State fMRI (DPARSF 2·2; http://restmri.net/forum/DPARSF), was used for the analysis of resting-state data. DPARSF is a plug-in software that runs on a matrix laboratory platform (MATLAB R2010b; MathWorks, Inc., Natick, MA, USA) and is based on Statistical Parametric Mapping (SPM8; http://www.fil.ion.ucl.ac.uk/spm). The preprocessing steps were as follows: the first 10 time points were discarded to avoid transient signal changes before the magnetization reached a steady state. Subjects with >1·5-mm maximum displacement in any dimension and 1·5° of angular motion during the entire fMRI were removed from the data analysis. No subjects were eliminated at this step. The head-motion courses were also compared among the four groups using repeated measures analysis of variance, which revealed no significant differences. The head-motion measurements were set as covariates for group-level comparisons. Slice timing and spatial realignment were performed. Following motion correction, all data were normalized to the Montreal Neurological Institute (MNI) space using echo planar imaging templates and resampling to 3-mm isotropic voxels. The normalized data were processed with the removal of linear trends and were temporally filtered (band pass, 0·01–0·08 Hz) to remove the effects of very-low-frequency drift and physiological high-frequency respiratory and cardiac noise. The structural MRI data were preprocessed and analyzed using Statistical Parametric Mapping software (SPM8, Wellcome Trust Centre for Neuroimaging, London, UK) implemented in MATLAB 7.11.0 (MathWorks, Natick, MA, USA). We used the VBM8 toolbox (http://dbm.neuro.uni-jena.de/vbm8/) with the longitudinal data approach batch. After a quality evaluation of the data, we manually reoriented the images to the anterior commissure. The VBM8 longitudinal batch had specific preprocessing steps for longitudinal data; the data from each subject were registered to the baseline image (or mean image), and spatial normalization parameters were estimated for only the baseline image and applied to all images. We used the “modulated normalized” and “non-linear only” options, resulting in tissue class images aligned with the template in which the voxel value was multiplied by the non-linear components. After segmentation, the GM and white matter volumes were entered into an iterative study-specific normalization procedure based on Diffeomorphic Anatomical Registration using Exponentiated Lie algebra. After normalization, the study-specific GM template was co-registered to a corresponding MNI space GM template using an affine transformation. GM segmentations for individual subjects were then normalized to the MNI space and modulated to preserve GM amounts during normalization and smoothed with an isotropic 6-mm full width at half-maximum Gaussian kernel.

2.5. fALFF Analysis

fALFF analysis was performed using the Resting-State fMRI Data Analysis Toolkit (REST 1·8; http://www.restfmri.net). The time series for each voxel was transformed to the frequency domain using fast

Fourier transform (FFT) (parameters: taper percent = 0 and FFT length = shortest), and the power spectrum was obtained, square-rooted and then averaged across 0·01 to 0·08 Hz at each voxel. This averaged square root was considered the ALFF. The fALFF was used as a normalized index of ALFF by providing the relative amplitude of the low-frequency domain against the entire spectrum of frequencies (Zou et al., 2008; Deng et al., 2016), which may effectively suppress physiological artifacts. Finally, all fALFF images were smoothed using a Gaussian kernel with a full width at a half-maximum of 6 mm.

2.6. Regions of Interest(ROI) Definition

Automated ROI was created using orthogonal contrasts in a factorial design. Exploratory ROIs were created by placing small spheres at local maxima in the statistical map. This was a post-processing method that used statistical parametric maps. To ensure that benefits from the proposed method were not due to the statistical parametric maps themselves, we performed two-sample *t*-tests or repeated measures analyses of variance based on the BOLD signal or GM volume changes to obtain the statistical parametric maps. The voxels in the statistical maps were then labeled by the appropriate ROIs drawn on the anatomical image.

2.7. Statistical Analysis

Data were entered the Statistical Package for the Social Sciences (SPSS ver. 19·0, Chicago, IL, USA) for statistical analysis. For visual function, a mixed design analysis of variance (ANOVA) was performed to evaluate the differences between the cataract and control groups and the changes observed before and after cataract surgery (binocular data). Independent sample *t*-tests were performed to examine the differences in age, sex, and MMSE scores between the cataract and control groups. For brain function, two-sample *t*-tests were performed to evaluate the differences in fALFF values between the cataract and control groups and the changes across time points after surgery. Repeated measures analyses of variance were used to evaluate the changes in MMSE scores and fALFF values preoperatively and postoperatively. The resulting statistical maps were set at a combined threshold of $P < 0·05$ with a minimum cluster size of 228 voxels, which corresponded to the corrected threshold of $P < 0·05$ determined by AlphaSim. For brain structure, two-sample *t*-tests were performed to evaluate the differences in GM volume between the cataract and control groups and the changes across time points after surgery (at a whole-brain threshold of $P < 0·05$, False Discovery Rate (FDR) corrected, voxels > 20), and repeated measures analyses of variance were used to analyze the changes before and after cataract surgery and the changes across time points after surgery (at a whole-brain threshold of $P < 0·01$, False Discovery Rate (FDR) corrected, voxels > 200).

3. Results

3.1. Demographics of the Patients in the Prospective, Controlled Clinical Trial

Twenty-six patients (13 males and 13 females) with ARC and 26 healthy controls without ARC, matched for age, sex, and education (a longer education duration is associated with a thicker cortex across several loci and a reduced risk of cognitive decline (Cox et al., 2016)), were recruited for our study. The mean age of the 26 patients in the cataract group was 63·81 ± 7·11 years (ranging from 47 to 72 years). The mean age of the 26 healthy subjects in the control group was 62·04 ± 6·83 years (ranging from 48 to 74 years). No significant differences were noted in terms of age, sex, and education between the cataract and control groups ($P > 0·05$, Cohen's d = 0·25; $P > 0·05$, Cramer's V = 0; $P > 0·05$, Cramer's V = 0).

In the cataract group, 8 patients were implanted with a single-focus intraocular lens (SIOL), and 18 patients were implanted with a multifocal intraocular lens (MIOL) (SI Appendix, Fig. S1). For the subgroup analysis between SIOLs and MIOLs, please refer to Supplementary Results.

3.2. Simultaneous Functional Decline and Structural Changes in the Eyes and Brains of Patients With ARC

3.2.1. Changes in Visual Function and Ocular Structure

The lenses of the cataract patients exhibited increased density and decreased transparency compared to those of the control group (SI Appendix, Fig. S2a). Additionally, the cataract group exhibited significantly lower UCDVA, logarithm of the minimum angle of resolution [LogMAR] than the control group (0·80 ± 0·42 vs. −0·02 ± 0·03, $P < 0·001$, Cohen's d = 0·275) (SI Appendix, Fig. S2b). Moreover, the cataract group showed a significantly longer peak time and lower P100 amplitude of PVEP than the control group (124·63 ± 14·59 vs. 106·80 ± 7·10 ms [peak time] ($P < 0·001$, Cohen's d = 1·55) and 7·95 ± 3·95 vs. 13·02 ± 6·80 μV [amplitude] ($P < 0·001$, Cohen's d = 0·911) (SI Appendix, Fig. S2c and d).

3.2.2. Changes in Neurocognitive Function

The MMSE is an international standard for evaluating intelligence state and cognitive impairment in patients with cognitive disorders (Predictors, 2017; Dixon et al., 2017b). The cataract group exhibited a significantly lower MMSE score (27·65 ± 1·47) than the control group (29·58 ± 0·86) ($P < 0·001$, Cohen's d = 1·60) (Fig. 2a). Next, we analyzed fALFF to quantify the intensity of regional spontaneous brain activity. In cataract patients, a decreased fALFF value was detected in areas related to vision and attention (superior occipital lobule and superior parietal lobule) and cognition (precuneus), with peak voxels detected in the inferior parietal lobule. By contrast, the fALFF value in the brainstem was significantly increased in the cataract group compared with that in the control group (Fig. 2b, c, d and Table 1). The fALFF values in the inferior parietal lobule of the control group and the cataract group were 0·15 ± 0·05 and 0·07 ± 0·06, respectively ($P < 0·05$, Cohen's d = 1·45). The fALFF values in the brainstem of the control group and the cataract group were −0·15 ± 0·09 and −0·06 ± 0·11, respectively ($P < 0·05$, Cohen's d = 0·90).

3.2.3. Changes in Brain Structure

GM is a major component of the central nervous system, mainly consisting of neuronal cell bodies and unmyelinated axons (Robertson, 2014). Changes in GM volumes are generally used to represent alterations in brain structure (Puri et al., 2008). The extracted GM value for the anterior cingulate gyrus (cognitive area) as ROI was significantly lower in the cataract group than that in the control group (0·35 ± 0·03 vs. 0·41 ± 0·03, $P < 0·05$, Cohen's d = 2·00) (Fig. 2e, f and Table 2).

3.3. Functional Visual Improvement After Optical Reconstruction

In the cataract group, the UCDVA values (0·80 ± 0·42) were significantly increased at 1 week (0·04 ± 0·08) ($P < 0·001$, Cohen's d = 2·51), 3 months (0·01 ± 0·07) ($P < 0·001$, Cohen's d = 2·62) and 6 months (0·01 ± 0·07, Cohen's d = 2·62) postoperatively. The best-corrected distance visual acuity (BCDVA) values (0·63 ± 0·41) were also significantly increased at 1 week (−0·04 ± 0·04), 3 months (−0·04 ± 0·04), and 6 months (−0·04 ± 0·04) postoperatively ($P < 0·001$, Cohen's d = 2·30) (SI Appendix, Fig. S3a, b, and SI Appendix, Table S1). Straylight measurement has been used to objectively evaluate the quality of vision (Van Den Berg et al., 2007). Compared with the value observed at 1 week postoperatively (1·39 ± 0·22), the retinal SV of log(s) was significantly decreased at 3 months (1·29 ± 0·18) ($P < 0·05$, Cohen's d = 0·50), and 6 months (1·23 ± 0·18) ($P < 0·05$, Cohen's d = 0·80) postoperatively, indicating a steady improvement in visual function (SI Appendix, Fig. S3c).

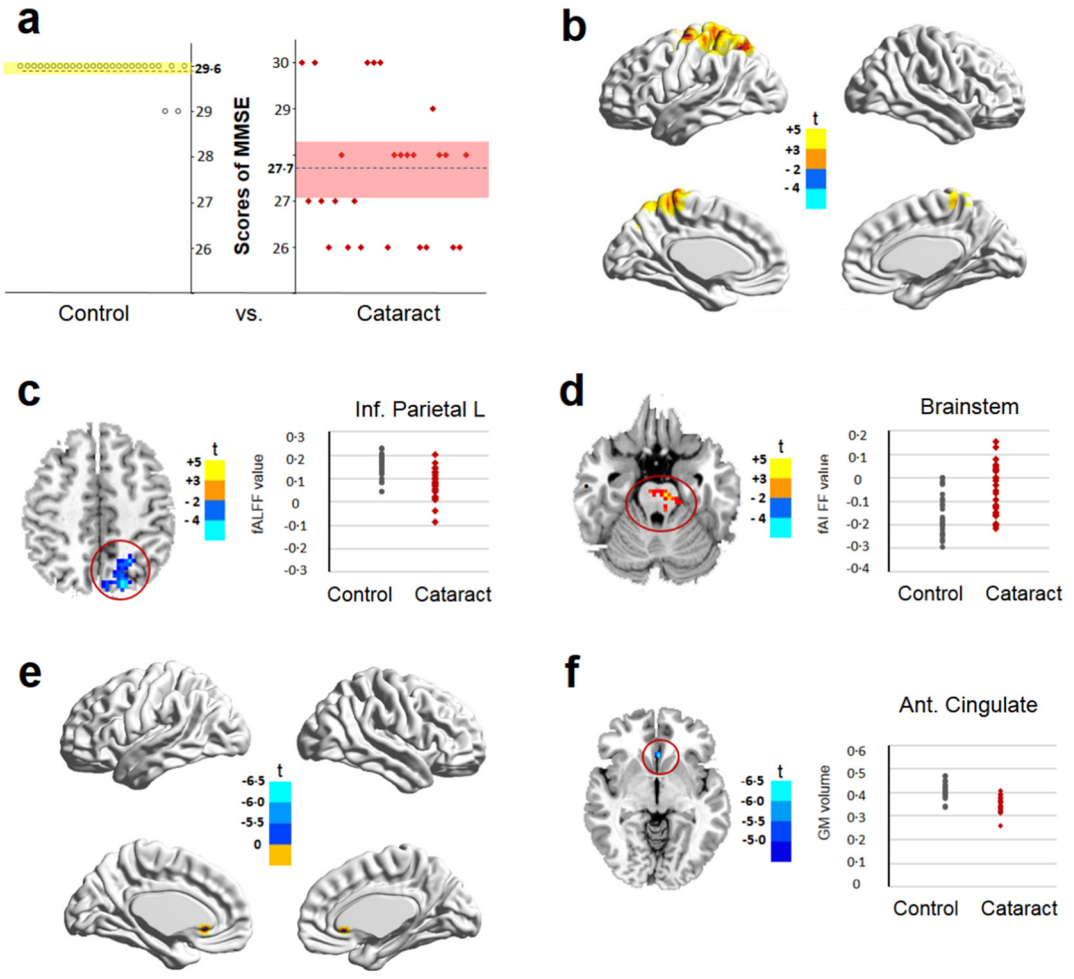

Fig. 2. Comparison of brain function and structure between the control and cataract groups before surgery. a, MMSE scores of the control and cataract groups were recorded ($P < 0{\cdot}001$, independent sample *t*-test). b, Surface maps show the changes in the fALFF values between the controls and patients with cataract (at a whole-brain threshold of $P < 0{\cdot}05$, AlphaSim corrected, voxels > 228, two-sample *t*-test). c, d, Slice overlays and plots represent the mean signal from the smoothed difference images for each cluster. Significant differences in signals between the control group and the cataract group are highlighted within the red circle. Blue and cyan reflect decreases in the superior parietal lobule, superior occipital lobule, and precuneus with peak voxels observed in the inferior parietal lobule. Red and yellow reflect increases in the brainstem, and *t* indicates the peak *t*-score value for the *t*-test. e, Surface maps show the changes in GM volume between the controls and the patients with cataract. f, Slice overlays and plots represent the mean signals from the smoothed difference images for each cluster. Significant differences in signals between the control group and the cataract group are highlighted within the red circle. Blue and cyan reflect decreases in the anterior cingulate gyrus, and *t* indicates the peak *t*-score value for the *t*-test. Notes: Dotted lines indicate the mean value; MMSE, Mini-Mental State Examination; fALFF, fractional amplitudes of low-frequency fluctuation; L, left; Inf, inferior; GM, grey matter; Ant. anterior.

Additionally, the P100 amplitude was significantly increased ($P < 0{\cdot}001$, Cohen's $d > 0{\cdot}8$) postoperatively, and the peak time was significantly decreased ($P < 0{\cdot}001$, Cohen's $d > 1{\cdot}2$) (SI Appendix, Fig. S3d and e). CS measurement is a sensitive method used to assess visual function in post-surgery cataract patients (Tzelikis et al., 2007). Compared with the value observed at 1 week postoperatively, the log CS value observed at 3 or 6 months postoperatively was significantly increased ($P < 0{\cdot}05$, Cohen's $d > 0{\cdot}5$) (SI Appendix, Fig. S3f). Collectively, these data showed that the visual function of cataract patients was significantly improved after surgery.

Table 1
Comparison of fALFF values between the control group and the cataract group before and after surgery.

Contrasts	Regions	BA	Cluster size (voxels)	MNI Coordinates			*t*-Score for peak voxels
				x	y	z	
Cataract vs. Control	Superior parietal lobule (L), superior occipital lobule, precuneus	7/19	304	−18	−78	48	−4·0796
	Brainstem		433	−6	−21	−24	3·8526
Post-1 w vs. Pre	–						
Post-3 m vs. Pre	Brainstem		957	18	−33	−36	−3·779
	Cerebellum posterior lobe (L)		247	−36	−60	−48	−3·3208
Post-6 m vs. Pre	Superior parietal lobule (L)	7/19	845	−18	−78	48	4·5655
	Brainstem		731	−6	−21	−24	−3·9227

Notes: A two-sample *t*-test with AlphaSim correction (>228 voxels) was used for the comparison between the control and cataract groups. The repeated measures analysis of variance test with AlphaSim correction (>228 voxels) was used for the comparison between preoperative and postoperative time points in the cataract group. A positive peak *t*-score value indicates an increase, and a negative value indicates a decrease. L, left; BA, Brodmann area; MNI, Montreal Neurological Institute.

Table 2
Comparison of GM volumes between the control group and the cataract group before and after surgery.

Contrasts	Regions	BA	Cluster size (voxels)	MNI coordinates			*t*-Score for peak voxels
				x	y	z	
Cataract vs. Control	Anterior cingulate gyrus	24	29	−1·5	24	−4·5	−6·3667
Post-1 w vs. Pre	–						
Post-3 m vs. Pre							
Post-6 m vs. Pre	Frontal Inf. Orb (R)	38/47	6433	34·5	24	−12	6·433
	Fusiform (L)	20/36	246	−25·5	−3	−40·5	4·9275
	Frontal Inf. Orb (L)	47	1957	−21	10·5	−19·5	6·0618
	Superior temporal gyrus (L)	21/22	1920	−49·5	−3	−4·5	6·159
	Frontal Med. Orb (L)	10	241	−4·5	54	−3	5·3166
	Calcarine (L)	18/19/30	506	−12	−61·5	10·5	5·052
	Calcarine (R)	18/30	216	18	−57	9	5·0549
	Anterior cingulate gyrus (R)	9/32	911	6	42	27	6·3945
	Middle frontal gyrus (L)	6/8/9	631	−43·5	12	42	5·989
	Middle frontal gyrus (R)	6/8/9	641	31·5	12	57	5·3926
	Middle cingulate gyrus (R)	31	660	1·5	−45	33	5·0194
	Precentral gyrus (R)	4	523	31·5	−25·5	57	4·9598
	Postcentral gyrus (L)	4	521	−46·5	−13·5	49·5	4·6004
	Precentral gyrus (L)	6	583	−30	−6	48	5·4285

Notes: The two-sample *t*-test with FDR correction (>20 voxels) was used for the comparison between the control and cataract groups. The repeated measures analysis of variance test with FDR correction (>200 voxels) was used for the comparison between preoperative and postoperative time points in the cataract group. A positive peak *t*-score value indicates an increase, and a negative value indicates a decrease. GM, grey matter; BA, Brodmann area; MNI, Montreal Neurological Institute. Pre, preoperative; Post-1 w, 1 week postoperatively; Post-3 m, 3 months postoperatively; Post-6 m, 6 months postoperatively; x, y, z: MNI coordinates of primary peak locations in the Talairach space; R, right; L, left; Frontal. Inf. Orb, inferior orbitofrontal cortex; Frontal. Med. Orb, medial orbitofrontal cortex.

3.4. Cognitive Functions and Brain Recovery After Visual Restoration

A previous study has shown that after cataract surgery, patients exhibited increased MMSE scores that were positively correlated with improvement of visual acuity (Ishii et al., 2008). Consistently, we observed that the registration, recall, attention, and calculation scores as well as the total MMSE scores were significantly increased at 3 and 6 months postoperatively compared with those at the preoperative time point (SI Appendix, Table S2). Additionally, we detected a significant decrease in the fALFF value in the brainstem and cerebellum regions 3 months postoperatively (Fig. 3a, b and Table 1). Six months postoperatively, the fALFF value was significantly increased in the vision-related areas (superior parietal lobule), but decreased in the brainstem (Fig. 3c and Table 1). Compared with the control group, an increased fALFF value in the brainstem but a decreased fALFF value in the superior parietal lobule (L) were noted at 1 week postoperatively (SI Appendix, Fig. S4a, SI Appendix, Table S3). Increased fALFF values in the precentral and postcentral gyrus were also detected 3 months postoperatively (SI Appendix, Fig. S4b, SI Appendix, Table S3). However, no significant differences were observed in the fALFF values between the patients at 6 months postoperatively and the controls (SI Appendix, Fig. S4c, SI Appendix, Table S3). These findings indicate that after cataract surgery, brain functions in cognitive and visual-related areas can be specifically enhanced and fully reversed to the normal level.

3.5. Structural Brain Recovery After Visual Restoration

No significant difference in GM volume was noted between the preoperative time point and 1 week and 3 months postoperatively (Fig. 4a, b and Table 2). However, significantly increased GM volume was observed 6 months postoperatively, specifically in the visual-related areas (calcarine), cognition-related areas (anterior cingulate gyrus), somatosensory-related areas (postcentral gyrus), somatic motor-related areas (precentral gyrus), and other areas (fusiform, inferior/middle frontal gyrus, and superior temporal gyrus) (Fig. 4c and Table 2), demonstrating that visual restoration could induce brain morphological changes at specific regions. Compared with the control group, significantly decreased GM volume was detected in the anterior cingulate gyrus at 1 week postoperatively (SI Appendix, Fig. S5a, SI Appendix, Table S4). However, no significant differences in GM volume were detected between the patients at 3 or 6 months postoperatively and the controls (SI Appendix, Fig. S5b, c, SI Appendix, Table S4). Collectively, these findings indicate that structural changes in the brains of cataract patients can be completely reversed after visual restoration.

3.6. Correlation Analysis Among Visual Function, Brain Function, and Brain Structure

To investigate the relationship between the changes in the eye and brain, we performed a partial correlation analysis among visual function (changes in BCDVA, UCDVA, and PVEP), brain function (changes in the fALFF value before and 6 months after surgery), and brain structure (changes in the extracted GM volume before and 6 months after surgery), with age as a controlling factor. When the fALFF value was extracted from the superior parietal lobule [L] of each patient, a statistically significant negative correlation was observed between the change in the peak time of P100 and the change in the fALFF value ($P = 0{\cdot}035$, $R = 0{\cdot}424$). (SI Appendix, Fig. S6a and SI Appendix, Table S5). Furthermore, a positive correlation was observed between the change in the fALFF value (superior parietal lobule (L)) and the change in GM volume (frontal. Med. Orb (L) and calcarine (R)) ($P < 0{\cdot}05$) (SI Appendix, Fig. S6b, c, SI Appendix, Table S6). These findings indicated a close relationship among visual function, brain function, and brain structure.

4. Discussion

The visual system and the brain seem to be more closely related than people ever thought. Previous studies have shown that cataract patients can present with an accelerated age-related decline in brain function (Rogers and Langa, 2010; Jefferis et al., 2011). However, whether optical reconstruction after cataract surgery can enhance brain function and structure is unclear. The present study is the first to show that cataract patients with reduced visual function presented a simultaneous decrease in brain function and GM volume. Cataract surgery not only restored visual function but also significantly improved brain function and increased GM volume in both visual- and cognitive-related regions (Fig. 5).

Several studies have reported improvements in cognition after cataract surgery based on subjective questionnaire investigations (Tamura et al., 2004; Ishii et al., 2008; Liu et al., 2005). Hiroki Tamura and colleagues enrolled patients with cognitive impairment and compared

their scores on the Revised Hasegawa Dementia Scale (RHD-S) before and after cataract surgery (Tamura et al., 2004). A significant improvement was noted, from 12·5 ± 5·3 points to 16·6 ± 6·2 points, 3·65 weeks after surgery (Tamura et al., 2004). Compared with the RHD-S, the MMSE is more suitable for cataract patients with visual impairments because it includes items evaluating reading and other visual-related abilities (Li et al., 2017). In our study, significantly lower MMSE scores were observed in the cataract group (27·65 ± 1·47) compared with those in the control group (29·58 ± 0·86). Moreover, the MMSE scores were significantly increased at 3 and 6 months after cataract surgery. Specifically, the registration, recall, attention and calculation scores were all improved, which is consistent with previous findings (Ishii et al., 2008). Nevertheless, repeated measurements of MMSE may result in being more familiar with questionnaire in cataract patients, leading to measurement bias, which should be interpreted with caution.

However, the subjective assessment of cognitive function under different pathophysiological conditions using the MMSE or other questionnaires has high inter-individual variation and lacks precision (Benedict and Brandt, 1992). A recent structural MRI study of unilateral cataract patients revealed that a regional expansion of GM volume occurs in the visual cortex area (V2) contralateral to the operated eye at 6 weeks after cataract surgery (Lou et al., 2013). However, the operation performed on unilateral cataract patients is not representative of an actual "sight restoration surgery", since the effects of visual restoration on visual cortex plasticity may be interceded by the relatively better visual acuity of the unoperated eye. Furthermore, the structural and functional alterations of other significant brain areas, such as the superior parietal lobule and anterior cingulate gyrus, after visual restoration remain unexplored. fMRI is a powerful tool for detecting subtle changes in the brain (Hazlett et al., 2017), and it can determine which brain regions are involved under critical conditions (Hoekzema et al., 2017). For example, cognitively impaired elderly people show decreased ALFF values primarily in the posterior cingulate cortex, precuneus, and right lingual gyrus(Liang et al., 2014) and exhibit neuropathological changes in the brain stem and limbic structures (Abulafia et al., 2017). The effect of congenital cataracts on the neural substrates of auditory processing was initially revealed in another study (Guerreiro et al., 2016). In this study, we show that cataract surgery is associated with substantial changes in brain function and GM volume in adults. The observed fALFF and GM volume increases were primarily located in the superior parietal lobule, calcarine, anterior cingulate gyrus, postcentral gyrus, and precentral gyrus of the cerebral cortex. These regions play essential roles in vision processing and various other high-order functions, such as cognition (Bush et al., 2000), somatic movement, and somatosensory processing (Inoue et al., 2013; Planetta and Servos, 2012).

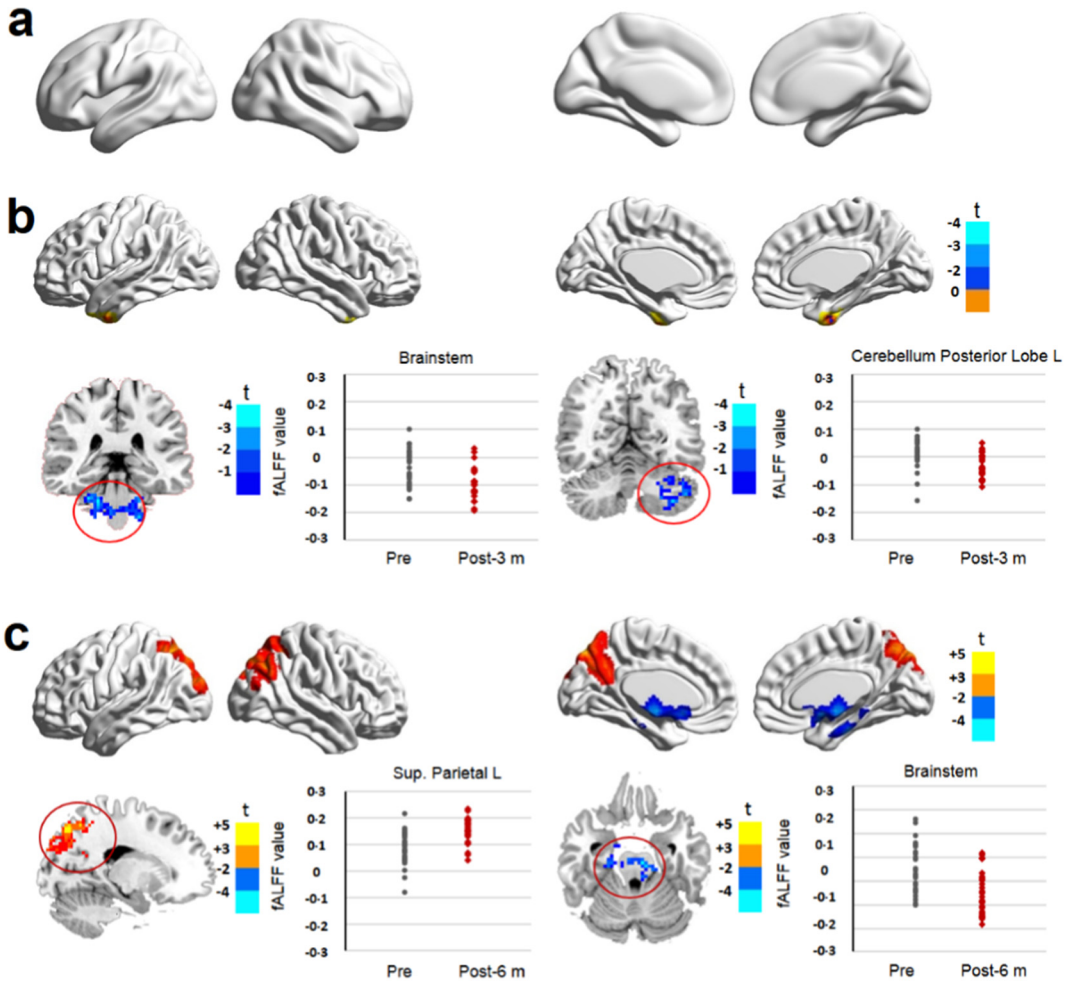

Fig. 3. Comparison of brain function in cataract patients before and after surgery. Surface maps show the fALFF value changes between preoperative and postoperative time points (at a whole-brain threshold of $P < 0·05$, AlphaSim corrected, voxels > 228, repeated measures analysis of variance). Slice overlays and plots represent the mean signals from the smoothed difference images for each cluster. Significant differences in signals are highlighted in the red circles. Blue and cyan reflect decreases. Red and yellow reflect increases, and *t* indicates the peak *t*-score value for the *t*-test. a, No significant difference in fALFF signals was detected between the preoperative and 1 week postoperative time points. b, The fALFF values were significantly decreased in the brainstem and cerebellum at 3 months postoperatively. c, The fALFF values were significantly decreased in the brainstem but increased in the superior parietal lobule 6 months postoperatively. Notes: L, left; Sup., superior.

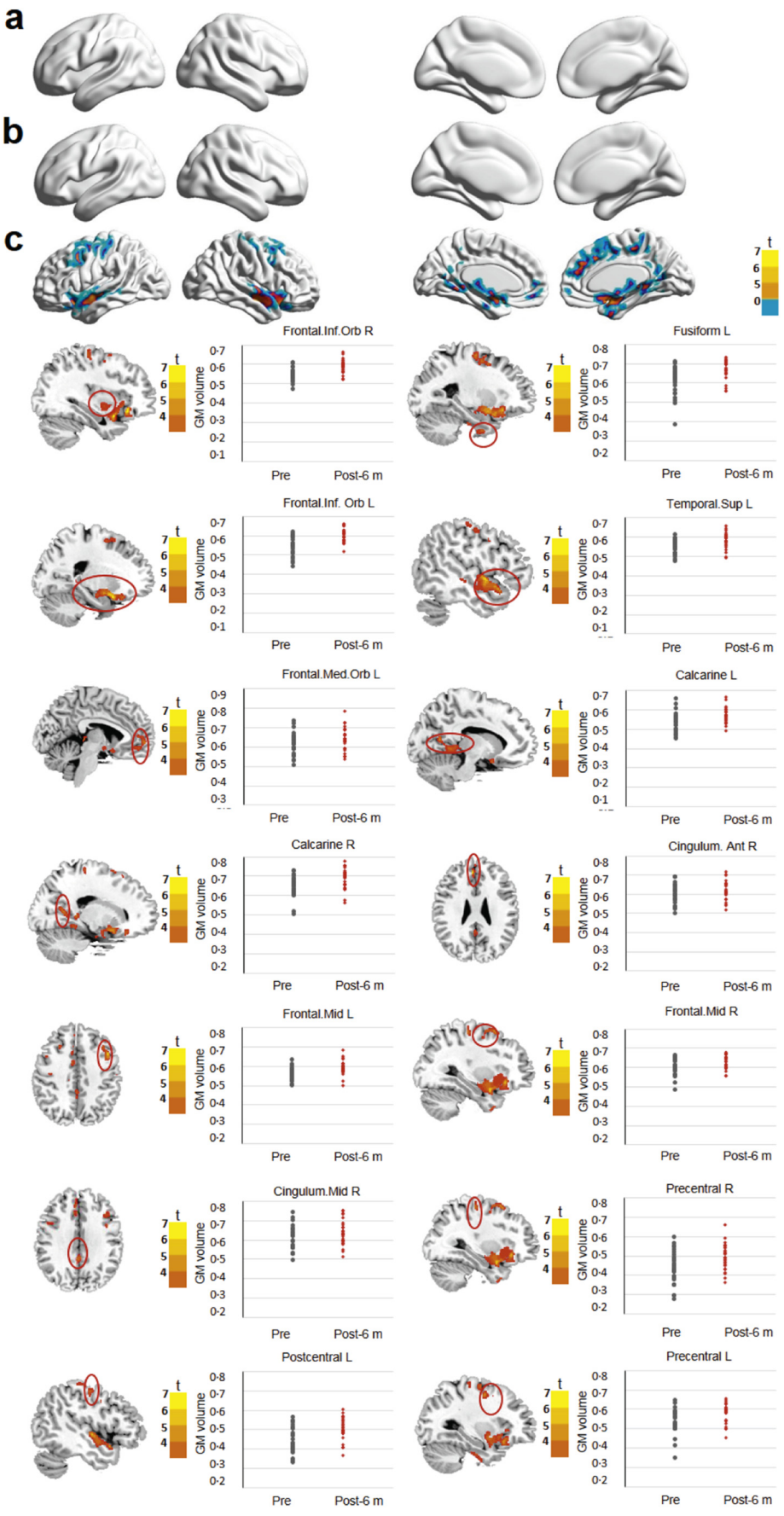
a
b
c
t
7
6
5
0
Frontal.Inf.Orb R
Fusiform L
Frontal.Inf. Orb L
Temporal.Sup L
Frontal.Med.Orb L
Calcarine L
Calcarine R
Cingulum. Ant R
Frontal.Mid L
Frontal.Mid R
Cingulum.Mid R
Precentral R
Postcentral L
Precentral L
GM volume
Pre
Post-6 m

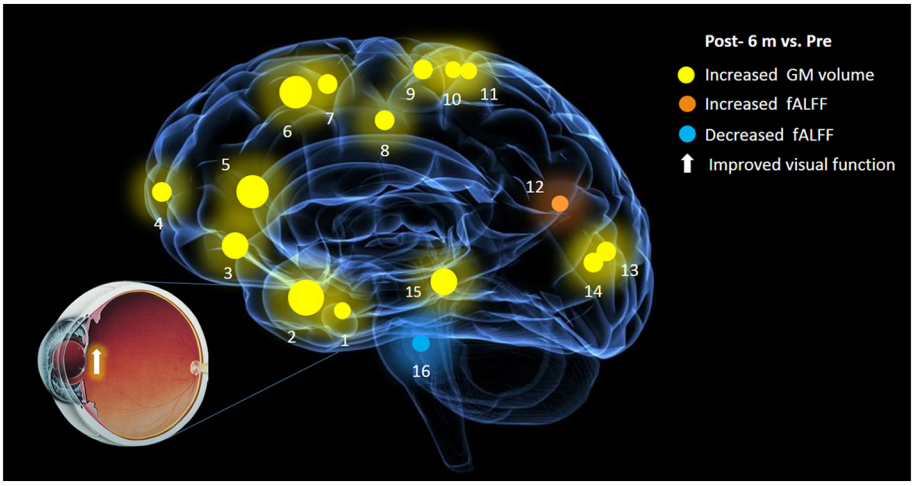

Fig. 5. Improvements in brain structure and function in cataract patients after visual restoration. Six months after cataract surgery, the GM volumes of the following regions were increased to various extents: 1-fusiform (L) (BA20/36, $t = 4{\cdot}928$), 2-frontal. Inf. Orb (R) (BA38/47, $t = 6{\cdot}433$), 3-frontal. Inf. Orb (L) (BA47, $t = 6{\cdot}062$), 4-frontal. Med. Orb (L) (BA10, $t = 5{\cdot}317$), 5-anterior cingulate gyrus (R) (BA9/32, $t = 6{\cdot}395$), 6-middle frontal gyrus (L) (BA6/8/9, $t = 6{\cdot}395$), 7-middle frontal gyrus (R) (BA6/8/9, $t = 5{\cdot}393$), 8-middle cingulate gyrus (R) (BA31, $t = 5{\cdot}020$), 9-precentral gyrus (L) (BA6, $t = 5{\cdot}429$), 10-precentral gyrus (R) (BA4, $t = 4{\cdot}960$), 11-postcentral gyrus (L) (BA4, $t = 4{\cdot}600$), 13-calcarine (R) (BA18/30, $t = 5{\cdot}055$), 14-calcarine (L) (BA18/19/30, $t = 5{\cdot}052$) and 15-superior temporal gyrus (L) (BA21/22, $t = 6{\cdot}159$). The fALFF of the 12-superior parietal lobule (L) (BA17/19, $t = 4{\cdot}566$) was increased after surgery, whereas the fALFF of the 16-brainstem ($t = -3{\cdot}923$) was decreased. Notes: The sizes of the spots represent the degree of quantitative changes; GM, grey matter; fALFF, the fractional amplitude of low-frequency fluctuations; frontal. Inf. Orb, inferior orbitofrontal cortex; frontal. Med. Orb, medial orbitofrontal cortex; R, right; L, left.

The mechanism underlying the alteration of brain function and structure after visual reconstruction has not been fully elucidated; however, gamma oscillations and photoreceptive retinal ganglion cells (pRGCs) have received increasing attention. Brain function can be directly affected by visual stimulation. For example, visual stimulation with a 40-Hz flicker elicits gamma oscillations in the visual cortex and reduces Aβ levels, which may have systemic effects on the brain and attenuate AD-related pathology (Iaccarino et al., 2016). Moreover, pRGCs detect light and arouse physiological and neurobiological responses through the non-visual pathway. Impaired pRGC photoreception and the subsequent disturbance of light-induced, sleep-related hippocampal function may aggravate problems such as insomnia and cognitive deficits. Aged crystalline lenses prominently block blue light, which is the exact effective light (wavelengths below 500 nm) required for unconscious photoreception (Brondsted et al., 2013; Kessel et al., 2010; Erichsen et al., 2015). Furthermore, patients with comorbid cognitive impairment and ARC tend to stay indoors, which exacerbates pRGC light deficiency and limits their exposure to beneficial visual stimuli. Therefore, patients with early cognitive impairment may benefit from early cataract extraction while their cooperation is still possible (Turner et al., 2010). In addition, cataract surgery may improve circadian photoreception, and IOLs that block only UV are more suitable than blue-blocking IOLs for improving cognition (Erichsen et al., 2015). However, further studies are required to dissect the molecular and cellular mechanisms underlying the improvements in brain function and structure after visual reconstruction.

In conclusion, our study demonstrated that the decline in visual function caused by ARC compromises brain function and structure and that these functional and structural changes can be reversed after cataract surgery. These findings provide further evidence that the integrity of the eye is essential for maintaining the function and structure of the brain within and beyond the primary visual pathway.

Authors' Contributions

H.T.L. designed the study. H.T.L. and W.R.C. conducted the experiments. H.T.L., L.Z., D.R.L., and W.C. contributed to data collection, analysis and interpretation and manuscript preparation. H.T.L. and L.Z. co-wrote the first draft of the report. K.C.C. critically reviewed the manuscript. H.T.L., D.R.L., Y.Z., C.C., and K.C.C. critically revised the manuscript. H.T.L., W.R.C., and Y.Z.L. obtained the research funding, coordinated the research and supervised the project. All authors reviewed the manuscript for important intellectual content and approved the final manuscript.

Competing Interests

The authors declare no competing financial interests.

Acknowledgments

We thank Zhiyun Yang, Jianping Chu, and Xinbei Li for providing technical assistance, and we also thank Yufeng Zang for critically reviewing the manuscript. This study was funded by the Natural Science Foundation of China (81570889, 81270980, and 91546101), the Science and Technology Program of Guangdong Province, China (2013B021800054, 2013B020400003, and 15570001), and the Clinical Research and Translational Medical Center Program in Guangzhou City (201505032017516). Haotian Lin is supported by the Guangdong Provincial Natural Science Foundation for Distinguished Young Scholars (2014A030306030) and Guangdong Province Universities and Colleges Pearl River Scholar Funded Scheme (2016-2018). The sponsors of the study played no role in study design, data collection, analysis, or interpretation, manuscript preparation, or the decision to submit the manuscript for publication.

Fig. 4. Comparison of brain GM volume in cataract patients before and after surgery. Surface maps show the changes in GM volume between preoperative and postoperative time points (at a whole-brain threshold of $P < 0{\cdot}01$, FDR corrected, voxels > 200, repeated measures analysis of variance). Slice overlays and plots represent the mean signals from the smoothed difference images for each cluster. Significant differences in the signals are highlighted in the red circles. Blue and cyan reflect decreases. Red and yellow reflect increases, and *t* indicates the peak *t*-score value for the *t*-test. a, b, No significant difference in the GM volume signal was detected between the preoperative time point and the 1-week (a) or 3-month (b) postoperative time points. c, Compared with the preoperative values, the GM volumes observed at 6 months after surgery were significantly increased in the calcarine, fusiform, anterior/middle cingulate gyrus, inferior/middle frontal gyrus, inferior/medial orbitofrontal cortex, and precentral/postcentral gyrus. Notes: Mid, middle; Sup, superior; R, right; Frontal. Inf. Orb, inferior orbitofrontal cortex; Frontal. Med. Orb., medial orbitofrontal cortex.

Appendix A. Supplementary data

Supplementary data to this article can be found online at https://doi.org/10.1016/j.ebiom.2018.03.002.

References

Abulafia, C., Duarte-Abritta, B., Villarreal, M.F., et al., 2017. Relationship between cognitive and sleep-wake variables in asymptomatic offspring of patients with late-onset Alzheimer's disease. Front. Aging Neurosci. 9, 93.

Asbell, P.A., Dualan, I., Mindel, J., Brocks, D., Ahmad, M., Epstein, S., 2005. Age-related cataract. Lancet (London, England) 365 (9459), 599–609.

Benedict, R.H., Brandt, J., 1992. Limitation of the mini-mental state examination for the detection of amnesia. J. Geriatr. Psychiatry Neurol. 5 (4), 233–237.

Brondsted, A.E., Lundeman, J.H., Kessel, L., 2013. Short wavelength light filtering by the natural human lens and IOLs—implications for entrainment of circadian rhythm. Acta Ophthalmol. 91 (1), 52–57.

Bush, G., Luu, P., Posner, M.I., 2000. Cognitive and emotional influences in anterior cingulate cortex. Trends Cogn. Sci. 4 (6), 215–222.

Cox, S.R., Dickie, D.A., Ritchie, S.J., et al., 2016. Associations between education and brain structure at age 73 years, adjusted for age 11 IQ. Neurology 87 (17), 1820–1826.

Dai, H., Morelli, J.N., Ai, F., et al., 2013. Resting-state functional MRI: functional connectivity analysis of the visual cortex in primary open-angle glaucoma patients. Hum. Brain Mapp. 34 (10), 2455–2463.

Deng, Y., Wang, Y., Ding, X., Tang, Y.Y., 2016. The relevance of fractional amplitude of low-frequency fluctuation to interference effect. Behav. Brain Res. 296, 401–407.

Dixon, J.S., Saddington, D.G., Shiles, C.J., Sreevalsan, K.P., Munro, C.A., Rosenberg, P.B., 2017a. Clinical evaluation of brief cognitive assessment measures for patients with severe dementia. Int. Psychogeriatr. 29 (7), 1169–1174.

Dixon, J.S., Saddington, D.G., Shiles, C.J., Sreevalsan, K.P., Munro, C.A., Rosenberg, P.B., 2017b. Clinical evaluation of brief cognitive assessment measures for patients with severe dementia. Int. Psychogeriatr. 1–6.

Erichsen, J.H., Brondsted, A.E., Kessel, L., 2015. Effect of cataract surgery on regulation of circadian rhythms. J Cataract Refract Surg 41 (9), 1997–2009.

Ferreira, S., Pereira, A.C., Quendera, B., Reis, A., Silva, E.D., Castelo-Branco, M., 2017. Primary visual cortical remapping in patients with inherited peripheral retinal degeneration. NeuroImage Clin. 13, 428–438.

Gottfried, A.W., Gilman, G., 1985. Visual skills and intellectual development: a relationship in young children. J. Am. Optom. Assoc. 56 (7), 550–555.

Guerreiro, M.J., Putzar, L., Roder, B., 2016. The effect of early visual deprivation on the neural bases of auditory processing. J. Neurosci. 36 (5), 1620–1630.

Hazlett, H.C., Gu, H., Munsell, B.C., et al., 2017. Early brain development in infants at high risk for autism spectrum disorder. Nature 542 (7641), 348–351.

Hoekzema, E., Barba-Muller, E., Pozzobon, C., et al., 2017. Pregnancy leads to long-lasting changes in human brain structure. Nat. Neurosci. 20 (2), 287–296.

Hsu, C.L., Best, J.R., Chiu, B.K., et al., 2016. Structural neural correlates of impaired mobility and subsequent decline in executive functions: a 12-month prospective study. Exp. Gerontol. 80, 27–35.

Iaccarino, H.F., Singer, A.C., Martorell, A.J., et al., 2016. Gamma frequency entrainment attenuates amyloid load and modifies microglia. Nature 540 (7632), 230.

Inoue, K., Nakanishi, K., Hadoush, H., et al., 2013. Somatosensory mechanical response and digit somatotopy within cortical areas of the postcentral gyrus in humans: an MEG study. Hum. Brain Mapp. 34 (7), 1559–1567.

Ishii, K., Kabata, T., Oshika, T., 2008. The impact of cataract surgery on cognitive impairment and depressive mental status in elderly patients. Am J. Ophthalmol. 146 (3), 404–409.

Jefferis, J.M., Mosimann, U.P., Clarke, M.P., 2011. Cataract and cognitive impairment: a review of the literature. Br. J. Ophthalmol. 95 (1), 17–23.

Kessel, L., Lundeman, J.H., Herbst, K., Andersen, T.V., Larsen, M., 2010. Age-related changes in the transmission properties of the human lens and their relevance to circadian entrainment. J Cataract Refract Surg 36 (2), 308–312.

Knezovic, A., Osmanovic-Barilar, J., Curlin, M., et al., 2015. Staging of cognitive deficits and neuropathological and ultrastructural changes in streptozotocin-induced rat model of Alzheimer's disease. J. Neural. Transm. (Vienna, Austria: 1996) 122 (4), 577–592.

Lai, S.W., Lin, C.L., Liao, K.F., 2014. Cataract may be a non-memory feature of Alzheimer's disease in older people. Eur. J. Epidemiol. 29 (6), 405–409.

Leguire, L.E., Algaze, A., Kashou, N.H., Lewis, J., Rogers, G.L., Roberts, C., 2011. Relationship among fMRI, contrast sensitivity and visual acuity. Brain Res. 1367, 162–169.

Li, Y., Fang, X., Zhao, W.G., Chen, Y., Hu, S.L., 2017. A risk factor analysis of cognitive impairment in elderly patients with chronic diseases in a Chinese population. Med. Sci. Monit. 23, 4549–4558.

Liang, P., Xiang, J., Liang, H., Qi, Z., Li, K., 2014. Alzheimer's disease NeuroImaging I. Altered amplitude of low-frequency fluctuations in early and late mild cognitive impairment and Alzheimer's disease. Curr. Alzheimer Res. 11 (4), 389–398.

Liu, D.T., Lam, S.P., Lam, D.S., Chan, W.M., 2005. Improvement in cognitive impairment after cataract surgery in elderly patients. J Cataract Refract Surg 31 (3), 457–458 (author reply 8).

Lou, A.R., Madsen, K.H., Julian, H.O., et al., 2013. Postoperative increase in grey matter volume in visual cortex after unilateral cataract surgery. Acta Ophthalmol. 91 (1), 58–65.

van der Meulen, I.J., Gjertsen, J., Kruijt, B., et al., 2012. Straylight measurements as an indication for cataract surgery. J Cataract Refract Surg 38 (5), 840–848.

Ochoa-Urdangarain, L.A., Rodriguez-Romero, A., Camacho-Caballero, O., et al., 2001. The fundus oculi in the hemiplegic patient. Rev. Neurol. 32 (4), 331–332.

Odom, J.V., Bach, M., Brigell, M., et al., 2016. ISCEV standard for clinical visual evoked potentials: (2016 update). Doc. Ophthalmol. 133 (1), 1–9.

Planetta, P.J., Servos, P., 2012. The postcentral gyrus shows sustained fMRI activation during the tactile motion aftereffect. Exp. Brain Res. 216 (4), 535–544.

Oh, P.J., 2017. Predictors of cognitive decline in people with cancer undergoing chemotherapy. Eur. J. Oncol. Nurs. 27, 53–59.

Puell, M.C., Benitez-del-Castillo, J.M., Martinez-de-la-Casa, J., et al., 2006. Contrast sensitivity and disability glare in patients with dry eye. Acta Ophthalmol. Scand. 84 (4), 527–531.

Puri, B.K., Counsell, S.J., Saeed, N., Bustos, M.G., Treasaden, I.H., Bydder, G.M., 2008. Regional grey matter volumetric changes in forensic schizophrenia patients: an MRI study comparing the brain structure of patients who have seriously and violently offended with that of patients who have not. BMC Psychiatry 8 (Suppl. 1), S6.

Robertson, S., 2014. What Is Grey Matter? https://www.news-medical.net/health/What-is-Grey-Matter.aspx, Accessed date: 10 July 2017

Rogers, M.A., Langa, K.M., 2010. Untreated poor vision: a contributing factor to late-life dementia. Am. J. Epidemiol. 171 (6), 728–735.

Tambini, A., Rimmele, U., Phelps, E.A., Davachi, L., 2017. Emotional brain states carry over and enhance future memory formation. Nat. Neurosci. 20 (2), 271–278.

Tamura, H., Tsukamoto, H., Mukai, S., et al., 2004. Improvement in cognitive impairment after cataract surgery in elderly patients. J Cataract Refract Surg 30 (3), 598–602.

Turner, P.L., Van Someren, E.J., Mainster, M.A., 2010. The role of environmental light in sleep and health: effects of ocular aging and cataract surgery. Sleep Med. Rev. 14 (4), 269–280.

Tzelikis, P.F., Akaishi, L., Trindade, F.C., Boteon, J.E., 2007. Ocular aberrations and contrast sensitivity after cataract surgery with AcrySof IQ intraocular lens implantation Clinical comparative study. J Cataract Refract Surg 33 (11), 1918–1924.

Van Den Berg, T.J., Van Rijn, L.J., Michael, R., et al., 2007. Straylight effects with aging and lens extraction. Am J. Ophthalmol. 144 (3), 358–363.

Wang, T., Li, Q., Guo, M., et al., 2014. Abnormal functional connectivity density in children with anisometropic amblyopia at resting-state. Brain Res. 1563, 41–51.

Zou, Q.H., Zhu, C.Z., Yang, Y., et al., 2008. An improved approach to detection of amplitude of low-frequency fluctuation (ALFF) for resting-state fMRI: fractional ALFF. J. Neurosci. Methods 172 (1), 137–141.